Self-cleaned electrochemical protein imprinting biosensor basing on a thermo-responsive memory hydrogel

Yubo Wei, Qiang Zeng, Qiong Hu, Min Wang, Jia Tao, Lishi Wang

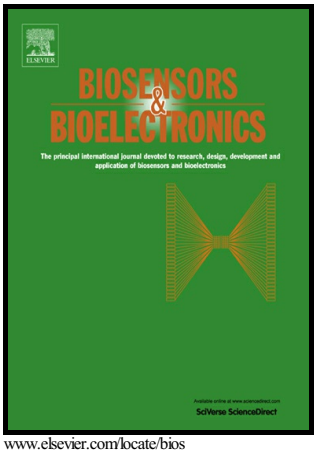

www.elsevier.com/locate/bios

PII: S0956-5663(17)30507-9
DOI: http://dx.doi.org/10.1016/j.bios.2017.07.049
Reference: BIOS9882

To appear in: *Biosensors and Bioelectronic*

Received date: 1 June 2017
Revised date: 8 July 2017
Accepted date: 19 July 2017

Cite this article as: Yubo Wei, Qiang Zeng, Qiong Hu, Min Wang, Jia Tao and Lishi Wang, Self-cleaned electrochemical protein imprinting biosensor basing on a thermo-responsive memory hydrogel, *Biosensors and Bioelectronic* http://dx.doi.org/10.1016/j.bios.2017.07.049

Self-cleaned electrochemical protein imprinting biosensor basing on a thermo-responsive memory hydrogel

Yubo Wei, Qiang Zeng, Qiong Hu, Min Wang, Jia Tao, Lishi Wang*

School of Chemistry and Chemical Engineering, South China University of Technology, Guangzhou 510641, People's Republic of China

*Corresponding author. wanglsh@scut.edu.cn

Abstract

Herein, the self-cleaned electrochemical protein imprinting biosensor basing on a thermo-responsive memory hydrogel was constructed on a glassy carbon electrode (GCE) with a free radical polymerization method. Combining the advantages of thermo-responsive molecular imprinted polymers and electrochemistry, the resulted biosensor presents a novel self-cleaned ability for bovine serum albumin (BSA) in aqueous media. As a temperature controlled gate, the hydrogel film undergoes the adsorption and desorption of BSA basing on a reversible structure change with the external temperature stimuli. In particular, these processes have been revealed by the response of cyclic voltammetry (CV) and electrochemical impedance spectroscopy (EIS) of electroactive $[Fe(CN)_6]^{3-/4-}$. The results have been supported by the evidences of scanning electron microscopy (SEM) and contact angles measurements. Under the optimal conditions, a wide detection range from 0.02 μmol L^{-1} to 10 μmol L^{-1} with a detection limit of 0.012 μmol L^{-1} (S/N=3) was obtained for BSA. This proposed BSA sensor also possesses high selectivity, excellent stability, acceptable recovery and good reproducibility in its practical applications.

Keywords: Molecularly imprinted polymers; Electrochemical biosensor; Bovine

serum albumin; Thermo-responsive memory hydrogel

Graphical abstract

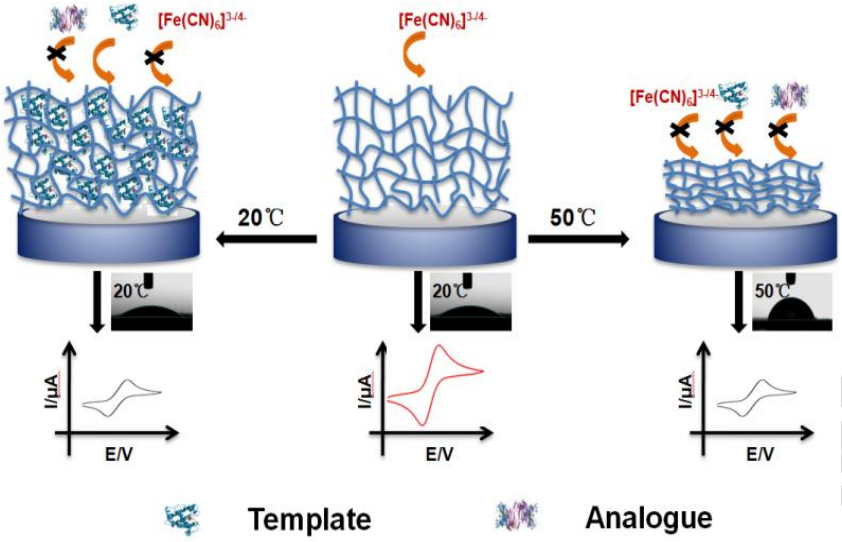

1. Introduction

Molecularly imprinted polymers (MIPs), which have selective recognition sites for target molecules, have been applied to various applications in biosensing (Ma et al., 2017a; Ma et al., 2017b), drug delivery (Culver et al., 2017), catalysis (Orozcoet al., 2013), solid-phase extraction (Tamayoet al., 2007), as well as diagnostics and therapeutics (Li et al., 2016a; Piletsky et al., 2006; Hillberg et al., 2005). MIPs have been successfully developed against a wide range of small protein molecules, such as lysozyme (Lyz, MW 23.8 kDa) (Pan et al., 2013a), ribonuclease A (RNase, MW 13.7 kDa) (Tan et al., 2007), and cytochrome C (Cyt C, MW 12.3 kDa) (Zhang et al., 2011). However, the molecular size, conformational flexibility, and solubility factors of the relatively large globular protein like bovine serum albumin (BSA) (MW 66.0 kDa) make it a challenging task to fabricate accessible binding sites with high specificity and affinity toward target proteins (Wulff et al., 2013; Li et al., 2014a; Chen et al., 2016). Many methods, such as micro-contact imprinting, imprinted hydrogel and epitope-mediated imprinting have been adopted to overcome these problems with improved the imprinted efficiency (Gai et al., 2011; Ran et al., 2012; Bakhshpour et

al., 2017; Pan et al., 2013b; Ma et al., 2017c; Li et al., 2016b), but difficulties in removing protein molecules and maintaining the stability of the imprinted film structures during the protein-imprinting process still seem to be huge. In the process of protein molecules eluting, washing solvents that perform strong interaction with polymers and result in the swelling of the coating are usually used for protein molecules release. This eluting method is somehow effective but inefficient. Therefore, it is of great necessity to develop a convenient method for the elution of protein in protein MIPs.

Stimuli-responsive MIPs not only can respond to external changes of stimuli such as temperature (Hua et al., 2008; Ambrosiniet al., 2013; Yang et al., 2016), solvent composition (Gong et al., 2017), pH (Karfa et al., 2016), light (Wei et al., 2015; Gong et al., 2016), and magnetic (Jiang et al., 2016), but also have molecular recognition ability for template molecules. In particular, the temperature-sensitive MIPs (TMIPs) consist of major thermo-sensitive monomer components that allow swelling and shrinking of the polymers and minor functional monomer components that capture target molecules (Liu et al., 2013). As a typical example, poly(*N*-isopropylacrylamide) (PNiPAAm) for the preparation of temperature responsive hydrogel can undergo reversible volume phase transition between their swollen and shrunk states around the lower critical solution temperature (LCST), leading the hydrophilic/hydrophobic conformation conversion of PNiPAAm in TMIPs when environmental temperature changed (Yu et al., 2016; Parlak et al., 2015; Ambrosiniet al., 2013). However, it is still rare to utilize TMIPs in electrochemical sensing, which may provide an effective way to illustrate processes of protein adsorption and desorption by investigation of interfacial electronic properties at an electrode surface under temperature stimulus.

In this study, a BSA TMIPs electrochemical biosensor has been developed with high sensitivity. With the thermo-responsive ability of TMIPs, the sensor gains the self-cleaning function to the template molecules by using potential cycling in a range of -0.8 V to +0.8 V for 14 cycles at 37 °C in a PBS buffer without the help of washing solvents. During the self-cleaning, BSA molecules can be efficiently removed from

the MIPs and the remained film still maintains a stably structure for further sensing application. The sensing process for BSA is achieved by a reversible MIPs structure change with the external temperature stimuli and monitored by the responses of cyclic voltammetry (CV) and electrochemical impedance spectroscopy (EIS). It is due to the reversibly controlled hydrophilic/hydrophobic conformation of the PNiPAAm in aqueous solutions by modulating environmental temperatures. To the best of our knowledge, this is the first report on the memory conformational MIPs electrochemical biosensor with the thermo-responsive self-cleaning function to the protein molecules of BSA.

2. Experimental section

2.1 Reagents and solutions

N-isopropylacrylamide (NiPAAm), acrylamide (AAm), methylene-*N*,*N*-bis(acrylamide) (MBAAm), bovine serum albumin (BSA), ammonium persulfate (APS), and *N,N,N′,N′*-tetramethylethylenediamine (TEMED) were purchased from TCI. All chemicals were analytical grade and used without further purification. All aqueous solutions were prepared using ultra-pure water (purified by 18.2 MU, Milli-Q, Millipore). 0.1 mol L^{-1} of PBS (pH=7.0) was prepared by mixing the stock solutions of NaH_2PO_4 and Na_2HPO_4, and used as working solution.

2.2 Apparatus and procedures

Electrochemical measurements of cyclic voltammetry (CV), electrochemical impedance spectroscopy (EIS) and differential pulse voltammetry (DPV) were performed on a CHI660C electrochemical workstation (Chenhua, Shanghai, China), equipped with a bare or modified glassy carbon electrode (GCE) as the working electrode, a saturated calomel reference electrode (SCE) and a platinum wire auxiliary electrode. A Kruss DSA25 contact angle measuring device was supplied by Kruss (Germany). Each sample was measured with a 2-μL drop of double-distilled water. The scanning electron micrographs were taken with field emission scanning electron microscopy (FE-SEM; Zeiss Ultra55, Germany). The compared BSA concentrations

in real samples were measured by a standard calibration curve method with a UV-3900H (Hitachi, Japan) spectrophotometer using 276 nm detection wavelength. The samples for SEM monitoring at 50 °C and 20 °C were prepared as follows: the TMIPs film were placed into liquid nitrogen immediately after being treated with the required temperatures for approximately 5 min to "freeze" the structures (Liu et al., 2012; Wang et al., 2014). And then the film were dehydrated with a LGJ-18S freeze drier (Beijing Songyuan Huaxing Technology) for 48 h until water content in the film was entirely removed.

2.3 Preparation of TMIPs film on electrode surface

The TMIPs electrochemical biosensor was prepared as following steps: (i) prior to fabrication of the biosensor, a bare GCE (3 mm diameter) was polished with 0.3 μm and 0.05 μm alumina powder, and then washed thoroughly with doubly distilled water in an ultrasonic bath. Then, the GCE was placed in a sealed wide-mouth bottle in a high-purity nitrogen atmosphere for 5 min; (ii) The pre-imprinted hydrogel was prepared by free radical polymerization, which contained 400.0 mg of NiPAAm as the temperature-responsive monomer, 5.0 mg of AAm as functional monomer, 5.0 mg of BSA as template, 5.0 mg MBAAm as a crosslinking agent, 5.0 mg mL^{-1} APS as an initiator, 5.0 μL TEMED as a promoter and 1.3 mL PBS buffer as solution. Functional monomers formed a stable complex with the amino and carboxyl groups of BSA via multiple-point electrostatic and hydrogen bonding interactions; (iii) 7.0 μL of the pre-imprinted hydrogel solution was then drop-casted onto the electrode surface under the protection of nitrogen before polymerization. After the polymerization under 20 °C for 30 min, the BSA-TMIPs film was formed on the electrode surface (BSA-TMIPs/GCE). The non-imprinted polymer film modified electrode (TNIPs/GCE) was prepared following the same steps mentioned above except adding any BSA.

In this work, the removal of BSA from BSA-TMIPs/GCE was conditioned in a PBS buffer using potential cycling in a range of -0.8 V to +0.8 V for 14 cycles (Scan rate: 100 mV s^{-1}) at 37 °C and the re-adsorption of BSA was conducted at 20 °C, which have been shown in Scheme S1 in details.

2.4 Electrochemical property measurements

CVs were recorded in the potential range from -0.2 V to +0.6 V in a PBS buffer containing 0.1 mol L^{-1} KCl and 5 mmol L^{-1} $[Fe(CN)_6]^{3-/4-}$ at a scan rate of 100 mV s^{-1}. DPV was conducted for quantitative analysis basing on the variation of the oxidation peak current of 5 mmol L^{-1} $[Fe(CN)_6]^{3-/4-}$ before and after being treated with BSA in a PBS buffer containing 0.1 mol L^{-1} KCl from -0.2 V to +0.6 V. The pulse amplitude, pulse period, and pulse width of DPV were 50 mV, 0.2 s, and 50 ms, respectively.

2.5 Real samples analysis

Real samples were prepared by 1.0 mL of liquid milk, bought from a local market, with 10.0 mL methanol solution (5%) followed by centrifugation at 25 °C, 5000 rpm for 20 min (Li et al., 2017). The supernatant was collected and diluted to 200.0 mL with a PBS buffer, and determined using the TMIPs/GCE.

3. Results and Discussion

3.1 Electrochemical behaviors of the TMIPs/GCE

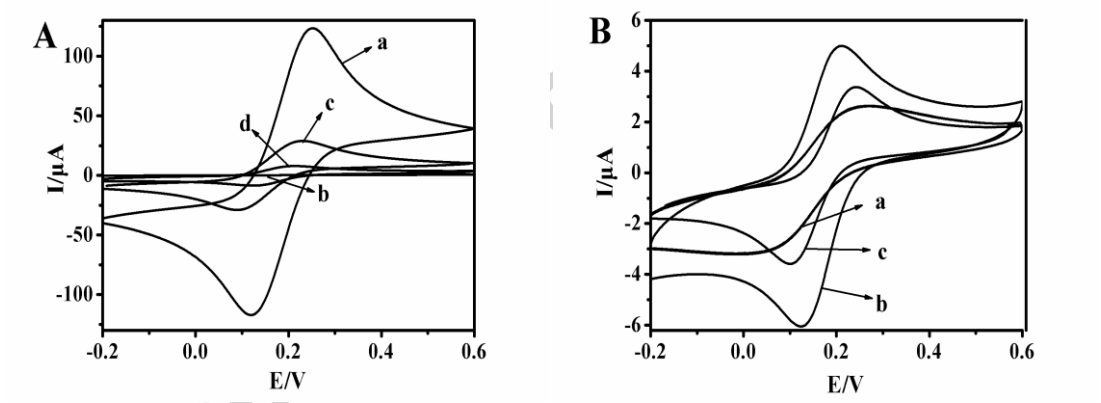

Fig. 1 (A) CV responses of (a) bare GCE; BSA-TMIPs/GCE before (b) and after (c) the removal of BSA at 37 °C; (d) TMIPs/GCE after incubated in 0.5 mL of 1.5 μmol L^{-1} BSA PBS buffer for 20 min; (B) CV responses of (a) TNIPs/GCE; (b) TNIPs/GCE treated at 37 °C; (c) TNIPs/GCE after incubated in 1.5 μmol L^{-1} BSA PBS buffer for 20 min.

As shown in Fig. 1A, comparing to the CV response of the bare GCE (curve a), the peak currents of the probe of $[Fe(CN)_6]^{3-/4-}$ were significantly reduced (curve b) after modification of the BSA-TMIPs on the GCE, indicating that the coating of a scarcely conductive and compact BSA-TMIPs film on the GCE surface blocks the

redox probe to reach the electrode surface. After the removal of BSA from the BSA-TMIPs/GCE using potential cycling in a range of -0.8 V to +0.8 V for 14 cycles (Scan rate: 100 mV s^{-1}) at 37 °C in a PBS buffer, the peak currents of the redox probe were increased (curve c). When the TMIPs/GCE was incubated in 0.5 mL of 1.5 μmol L^{-1} BSA solution for 20 min, the current response of the redox probe was decreased again (curve d). This result reveals that some cavities were recombined with BSA and the electron transfer of the redox probe was limited on the electrode surface.

CV responses of the TNIPs/GCE were also shown in Fig. 1B. After modification of the TNIPs film on the GCE surface, the electrode sensitivity was sharply reduced (curve a). Even treated under the same elution and incubation conditions as TMIPs/GCE, the TNIPs/GCE exhibits only slight changes on the peak currents of the redox probe. This phenomenon indicated that the TNIPs/GCE is lack of specific binding sites and cavities to BSA molecules.

3.2 The efficiency evaluation of self-cleaned BSA-TMIPs/GCE

Controlled experiments have been conducted to explore the self-cleaning behavior of BSA-TMIPs/GCE biosensor at 20 °C, 37 °C, 40 °C and 50 °C, which are related to the LCST of PNiPAAm in the BSA-TMIPs/GCE at 40 °C. The self-cleaning efficiency at different temperatures can be evaluated by the peak current variation (ΔI) of the redox probe.

Table 1 controlled experiments

Entry	T (°C)	Potential range	Cycles	Time (min)	ΔI (μA)	Fig. 2
1	20	-	-	17	10 ± 1	-
2	37	-	-	17	15 ± 2	-
3	40	-	-	17	7 ± 1	-
4	50	-	-	17	3 ± 1	-
5	37	-0.2 V to +0.6 V	65	17	38 ± 2	A
6	37	-0.8 V to +0.8 V	14	7	40 ± 2	B

Conditions: The BSA-TMIPs/GCE was conditioned in a PBS buffer containing 0.1 mol L^{-1} KCl and 5 mmol L^{-1} $[Fe(CN)_6]^{3-/4-}$; Scan rate:100 mV s^{-1}.

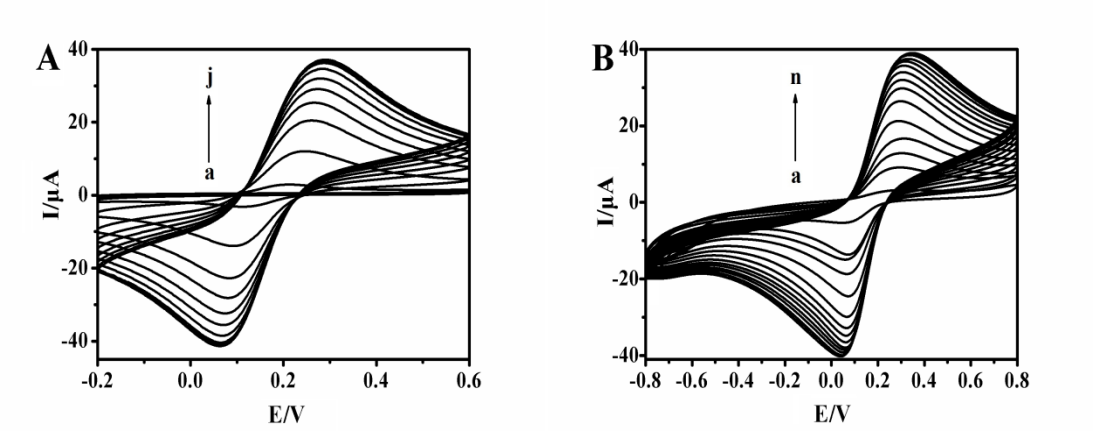

Fig. 2 CVs of BSA-TMIPs/GCE in the potential range from (A) -0.2 V to +0.6 V (a→j) (1, 7, 14, 21, 28, 35, 42, 49, 56, 65 cycle); (B) -0.8 V to +0.8 V (a→ n) (1→14 cycle) at 37 °C in a PBS buffer containing 0.1 mol L^{-1} KCl and 5 mmol L^{-1} $[Fe(CN)_6]^{3-/4-}$; Scan rate: 100 mV s^{-1}.

As shown in Table 1, when treated in 37 °C PBS buffer solution the *ΔI* of the redox probe for the BSA-TMIPs/GCE was significantly higher than those treated with 20 °C, 40 °C and 50 °C buffer (entries 1-4, Table 1). This observation is consistent with the temperature-dependent swollen and shrunk states of the PNiPAAm chains in TMIPs/GCE and the varied structure further results in the self-cleaning property. At 20 °C, the structure of the BSA-TMIPs/GCE has the greatest extent approaching to the original polymerization form. There is no external force to destroy the interaction between the templates and monomers. Close to the LCST at 37 °C, PNiPAAm chains in TMIPs start to conduct a hydrophilic/hydrophobic conformation conversion, which suppresses the interaction of hydrogen bonding between the templates and monomers and further leads BSA to be removed from the BSA-TMIPs/GCE. Temperatures higher or lower than the LCST, this structural conversion may be fully completed or not proceeded, allowing the remains of BSA in the structure. Furthermore, with additional potential cycling, *ΔI* is significantly enhanced (entries 5-6, Table 1). By contrast, a wider potential range (-0.8 V to +0.8 V) is responsible for accelerated destruction of the multiple-point electrostatic without the effects of oxygen and hydrogen evolution processes occurred at even higher and lower potentials, making the BSA removal much faster and more completed (Fig. 2A-B). Summing up all results, the self-cleaning conditions of BSA-TMIPs/GCE have been optimized at

37 °C with potential cycling in a range of -0.8 V to +0.8 V for 14 cycles (Scan rate: 100 mV s^{-1}).

3.3 Temperature-responsive property of the TMIPs/GCE

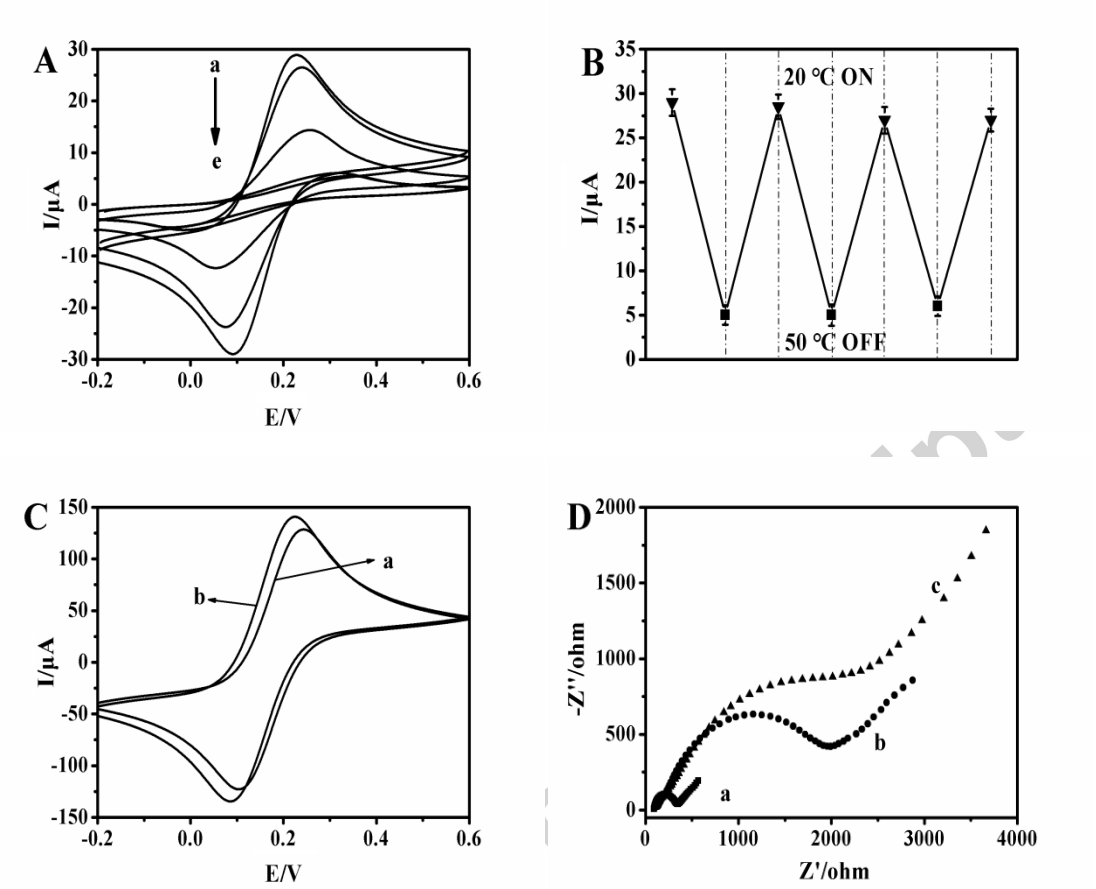

Fig. 3 (A) CV responses of the TMIPs/GCE in a PBS buffer at temperature (a) 20 °C, (b) 37 °C, (c) 40 °C, (d) 50 °C, and (e) 60 °C; (B) Variation of CV *Ipc* of the TMIPs/GCE for the temperature switched between 20 °C and 50 °C; (C) CV responses of bare GCE in a PBS buffer (a) 20 °C, (b) 50 °C; (D) EIS responses of the TMIPs/GCE in a PBS buffer (a) bare GCE, (b) 20 °C, (c) 50 °C at frequencies from 0.01 to 10^5 Hz.

In order to study the thermo-responsive properties of the TMIPs/GCE, BSA was initially removed from the template to form TMIPs/GCE by using potential cycling at 37 °C. As shown in Fig. 3A, the TMIPs/GCE demonstrated a dramatic decrease in the peak currents when the solution temperature increased from 20 °C to 60 °C and this process was fully reversible. Therefore, the TMIPs/GCE can present a stable ON–OFF switch property basing on its thermo-responsive behavior in particular, between 20 °C and 50 °C (Fig. 3B). However, the similar observation was not obtained at a

bare GCE (Fig. 3C), suggesting the thermo-responsive property specifically attributed to the MIPs. The observation on CVs was also consistent with the results of EIS (Fig. 3D), where the charge transfer ability of the redox probe to the electrode surface can be revealed by the interfacial electron transfer resistance (ETR) at different temperatures. They provide strong evidences that the TMIPs/GCE interfaces could effectively convert environmental information into electrochemical signals with a fast electrochemical switching behavior as well as excellent reversibility.

With the support of SEM, the thermo-responsive behavior of the TMIPs/GCE should be attributed to the structural changes of the temperature sensitive PNiAAm chains in the TMIPs film. At 20 °C, the TMIPs film showed a network like surface morphology with many roughly 10 μm diameter pores and channels (Fig. S1A-B). By contrast, after treated at 50 °C, the TMIPs film became more compact and the pore size decreased down to 2 μm (Fig. S1C-D). At a lower temperature, the PNiPAAm part in TMIPs forms hydrogen bonds with water molecules and takes swollen and expanded coil structure on the electrode surface. It would be convenient for the redox probe to diffuse through the film to the electrode surface, leading to the higher CV response and smaller interfacial ETR. When temperature increases, the hydrophobic interaction inside the film becomes overwhelming, resulting in the break of hydrogen bonds between PNiPAAm and water molecules and producing a contracted and compact globule structure. With the applications of CV and EIS, this structure can limit the access of the redox probe to the electrode surface, thus resulting in the smaller CV response and higher interfacial ETR.

The temperature dependent hydrophilic/hydrophobic conformation changes of the TMIPs film can be further confirmed by a surface wettability test using static water-contact angles measurements. The water-contact angle of the TMIPs film continuously increased from 24° to 56° and then to 76°, when environmental temperature varied from 20 °C to 40 °C then to 50 °C (Fig. S2 and the insets), indicating a thermo-responsive switching between hydrophilic and hydrophobic conformation. The LCST of TMIPs film can be thus estimated at around 40 °C from this curve which is consistent with the reported literatures for the LCST of PNiAAm

(Ji et al., 2016).

3.4 Adsorption properties of the TMIPs/GCE

The incubation time for the rebinding BSA is a critical parameter to evaluate the biosensor properties of the TMIPs/GCE. Fig. 4A represents the DPV peak currents variation (ΔI) of $[Fe(CN)_6]^{3-/4-}$ at the TMIPs/GCE and TNIPs/GCE before and after being interacted with BSA in case of incubation time range from 0 to 70 min. When the TMIPs/GCE was incubated in 0.5 mL of 1.5 μmol L^{-1} BSA PBS buffer from 0 min to 20 min, a sharply increase ΔI of the redox probe was observed obviously. With further increasing the incubation time from 20 min to 70 min, only a negligible increasing of the ΔI can be detected, which means that BSA have almost completely rebound to the template. Therefore, 20 min was adopted to be the optimal incubation time in the further experiments. For the TNIPs/GCE, however, binding capacity lower than TMIPs/GCE is due to non-specific adsorption occurred in the polymers.

As the consequence of thermo-sensitive conformation changes, the TMIPs/GCE exhibited different efficiency on the incubation of BSA at 20 °C, 37 °C, 40 °C and 50 °C. Using $[Fe(CN)_6]^{3-/4-}$ redox probe, ΔI by DPV was decreased significantly as temperature was increased from 20 °C to 50 °C (Fig. 4B). It may suggest that the film processes a conformational memory function at 20 °C and its imprint sites, conformational size, and functionality orientation have the greatest extent approaching to those originally polymerization formed, which is complementary to BSA. Therefore, the thermo-responsive rebinding capacity is primarily derived from the temperature-dependent volume phase transition of the TMIPs on GCE.

Associated with the self-cleaning ability, the TMIPs/GCE is able to perform the efficient BSA rebinding and releasing at 20 °C and 37 °C, respectively. During these processes, the TMIPs/GCE demonstrated satisfied durability. As revealed in Fig. 4C, more than 90% of affinity of the TMIPs/GCE toward the BSA was still maintained after three cycles, implying that the TMIPs/GCE possessed superior stability.

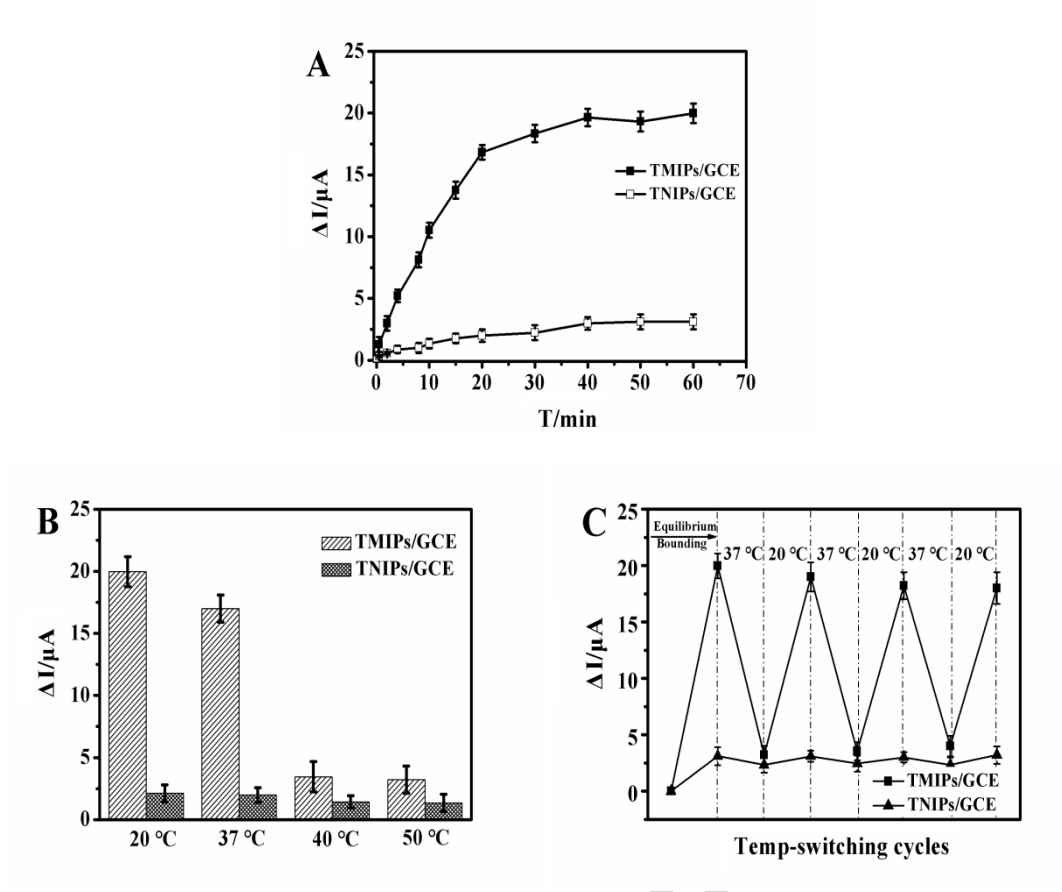

Fig. 4 (A) Incubation time on the peak current variations of $[Fe(CN)_6]^{3-/4-}$ for the TMIPs/GCE and TNIPs/GCE in 0.5 mL of 1.5 μmol L^{-1} BSA PBS buffer at 20 °C; (B) The peak current variations of the TMIPs/GCE and TNIPs/GCE after being incubated in 0.5 mL of 1.5 μmol L^{-1} BSA PBS buffer at 20 °C, 37 °C, 40 °C and 50 °C; (C) Thermoregulated release and uptake of 1.5 μmol L^{-1} BSA by the TMIPs/GCE and TNIPs/GCE.

3.5 Sensitivity, selectivity and application of the TMIPs/GCE

The determination of BSA by both TMIPs/GCE and TNIPs/GCE has been performed at 20 °C and 50 °C by DPV with $[Fe(CN)_6]^{3-/4-}$ redox probe. At 20 °C, TMIPs/GCE showed two linear calibration curves (Fig. 5A, curve a) when BSA re-bound to the imprinted cavities of TMIPs in a PBS buffer. Two linear regression equations were obtained at lower concentrations (0.02-1.5 μmol L^{-1}) as ΔI (μA) =-0.17+12.56 $C_{[BSA]}$ (R^2 = 0.996) with a detection limit of 0.012 μmol L^{-1} (S/N=3) and at higher concentrations (1.5-10 μmol L^{-1}) as ΔI (μA) =14.99+0.79 $C_{[BSA]}$ (R^2 = 0.997), respectively. The two calibration equations may suggest two types of binding sites in the imprinted polymer, where high and low affinity binding sites exist (Bai et

al., 2014). By contrast, TMIPs/GCE at 50 °C (Fig. 5A, curve b) and TNIPs/GCE (Fig. 5A, curve c) were not sensitive to BSA and the variation on ΔI is negligible, which is due to the lack of affinity in their conformations. To further evaluate the adsorption property of the TMIPs/GCE at 20 °C, Scatchard isotherms were applied to fit these static adsorption data as show in Fig. S3 (Gong et al., 2016) and the isotherms illustrate the batch-type rebinding assay of TMIPs/GCE with BSA. There are two linear components shown in the graph, indicating the presence of two different binding sites of specific binding and non-specific binding for BSA on the TMIPs/GCE. The specific binding constant k_d and the binding density Q_{max} were calculated to be 4.5 x10^{-5} mol L^{-1} and 10.4 mmol L^{-1}, respectively.

To evaluate the selectivity of the TMIPs/GCE, we chose some structurally similar as well as existent species covering wider molecular weight in serum with BSA (MW 66 kDa), such as human immunodeficiency virus p24 (HIV-p24, MW 24 kDa), human chorionic gonadotropin (HCG, MW 36 kDa), human serum albumin (HSA, MW 66 kDa), α-fetoprotein (AFP, MW 66 kDa) and carcino-embryonic antigen (CEA, MW 180 kDa) as potential interferents for comparison experiments. By DPV, the largest ΔI value of $[Fe(CN)_6]^{3-/4-}$ on the TMIPs/GCE was achieved toward BSA and 5.0, 6.1, 8.9, 8.9 and 10.6 times higher than that toward HIV-p24, HCG, HSA, AFP and CEA, respectively (Fig. 5B). However, there were no obvious differences between BSA and analogues for the TNIPs/GCE. The imprinted electrochemical biosensor also exhibited satisfactory stability. In fact, as much as 92% of the initial peak current was preserved after storage of the biosensor at 4 °C for 3 days. These results showed the TMIPs/GCE possessed high selectivity and stability for template protein BSA.

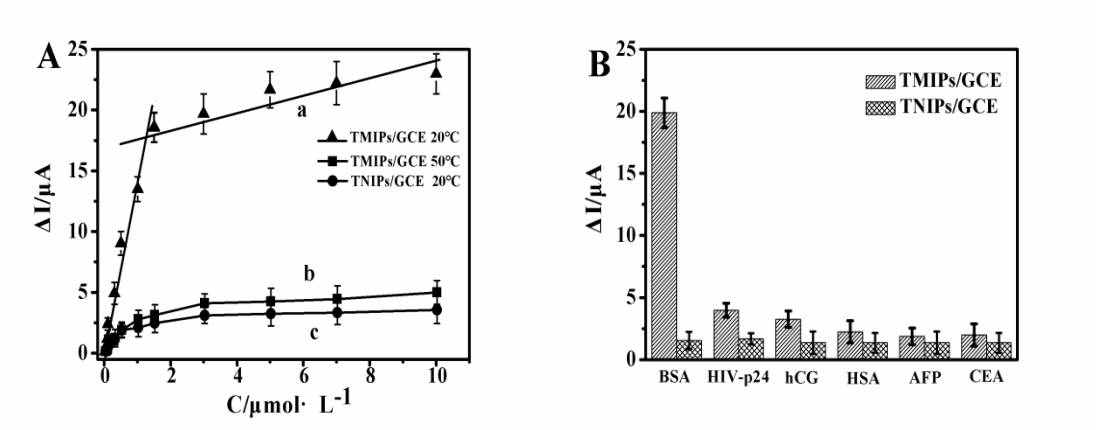

Fig. 5 (A) Calibration curves of the TMIPs/GCE and TNIPs/GCE toward BSA standards in a PBS buffer; (B) The selectivity of TMIPs/GCE and TNIPs/GCE for BSA, HIV-p24, HCG, HSA, AFP and CEA in a PBS buffer at 20 °C. The concentration of protein is 1.5 μmol L^{-1}.

The feasibility of the proposed sensor for measuring real samples was demonstrated by detecting BSA in daily milk products. As summarized in Table S1, the TMIPs/GCE was capable of detecting BSA with good recoveries varied from 98.2% to 103.1% for six measurements. Moreover, the experimental data have been compared with those obtained by an independent UV-Vis spectroscopic method (Li et al., 2014b; Liu et al., 2016) to verify the efficiency of the developed method. The comparison is also listed in Table S1 and it can be seen that there is no significant difference between the two series of results obtained by two methods. This observation indicates that the TMIPs/GCE possessed highly accurate, precise and it is potentially available for the analysis of real samples.

4. Conclusions

In summary, a sensitive and selective BSA TMIPs electrochemical biosensor was developed by free radical polymerization. Compared to the conventional biosensor, the proposed design presents two advantages: first, the biosensor gains the self-cleaning function to the BSA molecules by using potential cycling at 37 °C without the help of washing solvents; second, thermo-responsive MIPs in the biosensor are employed as temperature gates to control the adsorption and desorption of BSA at 20 °C and 37 °C while maintaining good stability. For the TMIPs sensors, the limitations of this method is that the TMIPs hydrogel are generally electrically

nonconductive, limiting their adoption in practical applications, but it is offer a promising supplementary for stimuli-responsive MIPs biosensing applications in particular, through an electrochemical approach.

Acknowledgements

This work was financially supported by the National Natural Science Foundation of China (Grant Nos. 21475046, 21427809, 21645004). We also acknowledge the Fundamental Research Funds for the Central Universities (No. 2015ZP028, 2017MS094).

References

Ambrosini, S., Beyazit, S., Haupt, K., Bui, B.T.S., 2013. Chem. Commun. 49, 6746-6748.

Bai, H.P., Wang, C., Chen, J., Peng, J., Cao, Q., 2015. Biosens. Bioelectron. 64, 352-358.

Bakhshpour, M., Özgür, E., Bereli, N., Denizli, A., 2017. Colloids Surf. B. 151, 264-270.

Chen, L., Wang, X., Lu, W., Wu, X., Li, J., 2016. Chem. Soc. Rev. 45, 2137-2211.

Culver, H.R., Clegg, J.R., Peppas, N.A., 2017. Acc. Chem. Res. 50 (2), 170-178.

Gong, C., Yang, Y., Yang, Y., Zheng, A., Liu, S., Tang, Q., 2016. J. Colloid Interface Sci. 481, 236-244.

Gong, C., Ou, X., Liu, S., Jin, Y., Huang, H., Tang, Q., Lam, M.H.-W., Chow, C., Tang, Q., 2017. Dyes and Pigments 137, 499-506.

Hua, Z.D., Chen, Z.Y., Li, Y.Z., Zhao, M.P., 2008. Langmuir 24 (11), 5773-5780.

Hillberg, A.L., Brain, K.R., Allender, C.J., 2005. Adv. Drug Delivery Rev. 57 (12), 1875-1889.

Jiang, H., Jiang, D., Shao, J., Sun, X., 2016. Biosens. Bioelectron. 75. 411-419.

Karfa, P., Roy, E., Patra, S., Kumar, D., Madhuri, R., Sharma, P.K., 2016. Biosens. Bioelectron. 78, 454-463.

Li, S., Cao, S., Whitcombe, M.J., Piletsky, S.A., 2014a. Prog. Polym. Sci. 39 (1), 145-163.

Li, X., Zhang, B., Li, W., Lei, X., Fan, X., Tian, L., Zhang, H., Zhang, Q., 2014b. Biosens. Bioelectron. 51, 261-267.

Li, W., Dong, K., Ren, J., Qu, X., 2016a. Angew. Chem. Int. Ed. 55, 8049-8053.

Li, S., Yang, K., Deng, N., Min, Y., Liu, L., Zhang, L., Zhang, Y., 2016b. ACS Appl. Mater. Interfaces 8 (9), 5747-5751.

Li, Y., Hsieh, C.-H., Lai, C.-W., Chang, Y.-F., Chan, H.-Y., Tsai, C.-F., Ho, J.-A., Wu, L.-C., 2017. Biosens. Bioelectron. 87, 142-149.

Liu, D., Liu, H., Hu, N., 2012. J. Phys. Chem. B 116 (5), 1700-1708.

Liu, H., Liu, X., Meng, J., Zhang, P., Yang, G., Su, B., Sun, K., Chen, L., Han, D., Wang, S., Jiang, L., 2013. Adv. Mater. 25, 922-927.

Liu, M., Pi, J., Wang, X., Huang, R., Du, Y., Yu, X., Tan, W., Liu, F., Shea, K.J., 2016. Anal. Chim. Acta 932, 29-40.

Ji, S., Li, N., Shen, Y., Li, Q., Qiao, J., Li, Z., 2016. Anal. Chim. Acta 909, 60-66.

Ma, Y., Shen, X.-L., Wang, H.-S., Tao, J., Huang, J.-Z., Zeng, Q., Wang, L.-S., 2017a. Anal. Biochem. 520 (1), 9-15.

Ma, Y., Shen, X.-L., Zeng, Q., Wang, H.-S., Wang, L.-S., 2017b. Talanta. 164 (1), 121-127.

Ma, X.-T., He, X.-W., Li, W.-Y., Zhang, Y.-K., 2017c. Sens. Actuators B 246, 879-886.

Orozco, J., Cortés, A., Cheng, G., Sattayasamitsathit, S., Gao, W., Feng, X., Shen, Y., Wang, J., 2013. J. Am. Chem. Soc. 135 (14), 5336-5339.

Piletsky, S.A., Turner, N.W., Laitenberger, P., 2006. Med Eng Phys. 28 (10), 971-977.

Pan, G., Guo, Q., Cao, C., Yang, H., Li, B., 2013a. Soft Matter 9, 3840-3850.

Pan, G., Guo, Q., Ma, Y., Yang, H., Li, B., 2013b. Angew. Chem. Int. Ed. 52, 6907-6911.

Parlak, O., Ashaduzzaman, M., Kollipara, S.B., Tiwari, A., Turner, A.P.F., 2015. ACS Appl. Mater. Inter. 7 (43), 23837-23847.

Gai, Q.-Q., Qu, F., Zhang ,T., Zhang, Y.-K., 2011. J. Chromatogr. A 1218 (22), 3489-3495.

Ran, D., Wang, Y., Jia, X., Nie, C., 2012. Anal. Chim. Acta 723, 45-53.

Tan, C.J., Tong, Y.W., 2007. Anal. Chem. 79 (1), 299-306.

Tamayo, F.G., Turiel, E., Martín-Esteban, A., 2007. J. Chromatogr. A 1152, 32-40.

Wulff, G., 2013. Microchim. Acta. 180 (15), 1359-1370.

Wang, P., Liu, S., Liu, H., 2014. J. Phys. Chem. B 118 (24), 6653-6661.

Wei, Y., Tang, Q., Gong, C., Lam, M.H.-W., 2015. Anal. Chim. Acta 900, 10-20.

Yang, C., Yan, X., Guo, H., Fu, G., 2016. Biosens. Bioelectron. 75, 129-135.

Yu, X., Lian, W., Zhang, J., Liu, H., 2016. Biosens. Bioelectron. 80, 631-639.

Zhang, W., He, X.-W., Chen, Y., Li, W.-Y., Zhang, Y.-K., 2011. Biosens. Bioelectron. 26 (5), 2553-2558.

Highlights

- A self-cleaned electrochemical BSA imprinting biosensor basing on a thermo-responsive memory hydrogel was proposed, presenting a novel self-cleaned ability for BSA in aqueous media.
- The advantages of the self-cleaned BSA-imprinted electrochemical biosensor are that not only quickly remove the BSA molecular but also could maintain the stability of the imprinted films structure during the BSA-imprinting sensing.
- The proposed biosensor used as a temperature gate to control the adsorption and desorption of bovine serum albumin.